

BaM(BS₃)S (M = Sb, Bi): Two New Thioborate Compounds with One-Dimensional Polymeric Chain Structure

Lei Geng,^{†‡} Wen-Dan Cheng,^{*†} Wei-Long Zhang,^{†‡} Chen-Sheng Lin,[†] Hao Zhang,[†] Ye-Yu Li,^{†‡} and Zhang-Zhen He[†]

[†]State Key Laboratory of Structural Chemistry, Fujian Institute of Research on the Structure of Matter, Chinese Academy of Sciences, Fuzhou 350002, P. R. China, and [‡]Graduate School of the Chinese Academy of Sciences, Beijing, 100039, P. R. China

Received March 21, 2010

Two new quaternary thioborate compounds with strongly one-dimensional growth, BaSb(BS₃)S and BaBi(BS₃)S, have been synthesized using the conventional solid state reaction method in closed tubes at 1100 K. The single crystal X-ray diffraction analysis has shown that compound BaSb(BS₃)S crystallizes in space group *Pnma* of the orthorhombic system with unit cell parameters of $a = 9.6898(15)$ Å, $b = 6.2293(13)$ Å, $c = 11.670(2)$ Å, $V = 704.4(2)$ Å³, and $Z = 4$, while compound BaBi(BS₃)S crystallizes in space group *C2/m* with unit cell parameters of $a = 14.9890(17)$ Å, $b = 6.2457(6)$ Å, $c = 7.5591(9)$ Å, $\beta = 101.604(5)^\circ$, $V = 693.19(13)$ Å³, and $Z = 4$. The two compounds both crystallize in the structure of infinite one-dimensional chains with [BS₃]³⁻ trigonal plane coordination alternately bridged by [MS₃]³⁻ (M = Sb, Bi) trigonal pyramids through sharing two sulfur atoms along the crystallographic *b* axis. First-principles electronic structure calculations performed with the density functional theory (DFT) method show that the calculated band gaps of BaSb(BS₃)S and BaBi(BS₃)S are 2.29 and 2.16 eV, respectively, which are in good agreement with the experimental values estimated from UV–vis absorption spectra using the Kubelka–Munk equation, and the observed absorption peak is assigned as charge transfers from S-3p states to Sb-5p (Bi6p) states.

Introduction

Over the past two decades, thioborates have attracted considerable interest owing to their rich structural varieties and chemical particularities. Among dozens of thioborates structurally determined so far, several compounds have been found to have a [BS₃]³⁻ trigonal plane or [BS₄]⁵⁻ tetrahedral units in the ternary A–B–S (A = Li,¹ Na,² K,² Rb,^{2,3} Cs,³ Tl,³ Ba,^{4,5} etc.) system. The combinations of the above two kinds of structural units in thioborates can also result in the formation of various chalcogenoborate anions groups, such as [B₃S₆]³⁻, [B₄S₁₀]⁸⁻, [B₁₀S₁₆S_{4/2}]⁶⁻, etc. The acentric planar or tetrahedral anionic groups in thioborates, if they crystallize in noncentrosymmetrical space groups, may become potentially useful materials, especially in the field of

nonlinear optical and piezoelectric applications.^{6,7} In the case of [BS₃]³⁻ units, outer 2s²2p¹ electrons on boron atoms hybridize into three planar sp² orbitals and form σ bonds with three corner sulfur atoms. The remaining p_z orbitals on the three sulfur atoms further form delocalized π orbitals perpendicular to the [BS₃]³⁻ plane. The π -conjugated electrons delocalized on the [BS₃]³⁻ or [B₃S₆]³⁻ planes are very susceptible to the external electric field applied and strongly enhance the first and higher order polarizations, especially when these acentric blocks arrange toward the same direction in the crystal. Recently, second harmonic generation (SHG) has been displayed in thioborate crystal Zn_xBa₂B₂S_{5+x} ($x \approx 0.2$) for the first time, which exhibited relatively strong SHG efficiency (about 50 times that of α -SiO₂) arising from the asymmetric [BS₃]³⁻ anionic group.⁸

As the demands for new nonlinear optical crystals possessing larger nonlinearity and wider transmission efficiency in the mid-infrared band have become more and more pressing, thioborates may be potentially applied as one kind of compound which could have both large nonlinearities and a high laser damage threshold. However, preparation of single crystals of thioborates is difficult due to the high chemical activity of boron sulfide, which would evaporate

*To whom correspondence should be addressed. E-mail: cwd@fjirsm.ac.cn.

(1) Hiltmann, F.; Jansen, C.; Krebs, B. *Anorg. Allg. Chem.* **1996**, *622*, 1508.

(2) Kuchinke, J.; Jansen, C.; Lindemann, A.; Krebs, B. *Z. Anorg. Allg. Chem.* **2001**, *627*, 896.

(3) Lindemann, A.; Küper, J.; Hamann, W.; Kuchinke, J.; Köster, C.; Krebs, B. *J. Solid State Chem.* **2001**, *157*, 206.

(4) Kim, Y.; Martin, S. W. *Inorg. Chem.* **2004**, *43*, 2773.

(5) Hammerschmidt, A.; Dösch, M.; Wulff, M.; Krebs, B. *Z. Anorg. Allg. Chem.* **2002**, *628*, 2637.

(6) Becker, P. *Adv. Mater.* **1998**, *10*, 979.

(7) Jung, H. R.; Jin, B. M.; Cha, J. W.; Kim, J. N. *Mater. Lett.* **1997**, *30*, 41.

(8) Kim, Y.; Martin, S. W.; Ok, K. M.; Halasyamani, P. S. *Chem. Mater.* **2005**, *17*, 2046.

all around the container under high temperatures and react with silica dioxide. Consequently, only a relatively small number of thioborate crystals were structurally determined, and most of them were ternary alkali- or quaternary alkali-earth-containing compounds. The stereochemically active lone pair electrons on Sb^{3+} or Bi^{3+} were reported to help the formation of compounds with noncentrosymmetric structures, which may subsequently possess interesting physical properties such as SHG effects.^{9,10} Therefore, we attempted to explore the Ba–M–B–S (M = Sb, Bi) systems and obtained two quaternary thioborate compounds: $\text{BaM}(\text{BS}_3)_2$ (M = Sb, Bi), which incorporate the $[\text{BS}_3]^{3-}$ triangle plane ring and $[\text{SbS}_3]^{3-}$ (or $[\text{BiS}_3]^{3-}$) trigonal pyramid geometry together through sharing neighbored sulfur atoms with each other and form one-dimensional infinite chains along the crystallographic *b* direction. This kind of crystal structure has been reported in BaBiBO_4 analogous materials,¹¹ but it is found for the first time in thioborate systems. Here, we report the synthesis of the two quaternary thioborates, $\text{BaSb}(\text{BS}_3)_2$ and $\text{BaBi}(\text{BS}_3)_2$, and their crystal structure determination and electronic structure calculations using the plane-wave pseudopotential approach within the density functional (DFT) formalism.

Experimental Section

Synthesis. A quartz glass ampule is usually employed in sulfide synthesis, but it will be attacked by boron sulfide owing to the latter's high chemical reactivity, especially under high temperatures above 650 K.^{3,12,13} When this happens, B–Si exchange will bring impurities of B_2O_3 and SiS_2 and prevent further formation of thioborates.⁵ Accordingly, we adopt graphite crucibles as reagent containers in the following experiments. Reactants were loaded in previously dried graphite crucibles, which were then sealed in fused quartz tubes under a vacuum for further high temperature reaction in the next step.

The starting materials used are listed as follows: elementary bismuth (99.99%), elementary antimony (99.99%), amorphous boron (99.9%), barium sulfide (99.7%), and sublimed sulfur (99.5%). According to the molar ratios of 1:1:1:3 BaS/Bi(Sb)/B/S, stoichiometric mixtures of 1 g were well mixed and loaded in graphite ampules, which were then placed in predried silica tubes and sealed under 10^{-2} Pa. The above samples were placed into a vertical furnace and heated to 800 K (holding for 20 h) at a rate of 100 K/h, then heated to 1100 K at a rate of 30 K/h (holding for 10 h), and then slowly cooled down to room temperature within 200 h. Colorless crystals of $\text{BaSb}(\text{BS}_3)_2$ and orange-yellow $\text{BaBi}(\text{BS}_3)_2$ were yielded, and both of them are transparent and needle-shaped. $\text{BaSb}(\text{BS}_3)_2$ is relatively stable in the air for several weeks, while $\text{BaBi}(\text{BS}_3)_2$ gradually becomes dark and opaque after three days.

Crystal Structure Determination. Colorless and orange-yellow needle-like single crystals of $\text{BaSb}(\text{BS}_3)_2$ ($0.20 \times 0.16 \times 0.10 \text{ mm}^3$) and $\text{BaBi}(\text{BS}_3)_2$ ($0.20 \times 0.10 \times 0.10 \text{ mm}^3$) were prepared for single crystal structure determination. The crystal diffraction data of $\text{BaSb}(\text{BS}_3)_2$ were collected on a Rigaku Saturn70 diffractometer equipped with graphite monochromatized Mo $K\alpha$ radiation

Table 1. Crystallographic Data and Structural Refinement Details for $\text{BaSb}(\text{BS}_3)_2$ and $\text{BaBi}(\text{BS}_3)_2$

| formula | $\text{BaSb}(\text{BS}_3)_2$ | $\text{BaBi}(\text{BS}_3)_2$ |
|---------------------------------------|-------------------------------|--------------------------------|
| fw | 398.14 | 485.37 |
| cryst syst | orthorhombic | monoclinic |
| space group | <i>Pnma</i> (no. 62) | <i>C2/m</i> (no. 12) |
| <i>a</i> (Å) | 9.6898(15) | 14.9890(17) |
| <i>b</i> (Å) | 6.2293(13) | 6.2457(6) |
| <i>c</i> (Å) | 11.670(2) | 7.5591(9) |
| β (deg) | 90 | 101.604(5) |
| <i>V</i> (Å ³), <i>Z</i> | 704.4(2), 4 | 693.19(13), 4 |
| λ (Å) | 0.71073 | 0.71073 |
| temperature (K) | 293(2) | 293(2) |
| calcd density (g cm ⁻³) | 3.754 | 4.651 |
| cryst dimensions (mm ³) | $0.2 \times 0.16 \times 0.10$ | $0.20 \times 0.10 \times 0.10$ |
| θ range (deg) | $2.73 \leq \theta \leq 27.48$ | $2.75 \leq \theta \leq 27.47$ |
| <i>F</i> (000) | 704 | 832 |
| absorption correction | Multiscan | Multiscan |
| μ (mm ⁻¹) | 10.452 | 32.074 |
| reflns, total/unique | 4596/817 | 2669/859 |
| <i>R</i> (int) | 0.0329 | 0.044 |
| extinction coefficient | 0.0000 | 0.0039(3) |
| R_1^a/wR_2^b , for $I > 2\sigma(I)$ | 0.0171/0.0415 | 0.0325/0.0805 |
| R_1^a/wR_2^b , for all data | 0.0182/0.0420 | 0.0344/0.0811 |
| goodness-of-fit on F^2 | 1.104 | 1.135 |

$$^a R_1 = \frac{\sum w|F_o| - |F_c|}{\sum w|F_o|}, \quad ^b wR_2(F_o^2) = \frac{[\sum w(F_o^2 - F_c^2)^2]}{\sum w(F_o^2)^2}^{1/2}$$

($\lambda = 0.71073 \text{ \AA}$) and a CCD area detector, and the data of $\text{BaBi}(\text{BS}_3)_2$ were collected on a Rigaku Mercury CCD diffractometer with graphite monochromatized Mo $K\alpha$ radiation ($\lambda = 0.71073 \text{ \AA}$). Intensity data were collected at 293 K, and the exposure time is 3 and 10 s every frame for $\text{BaSb}(\text{BS}_3)_2$ and $\text{BaBi}(\text{BS}_3)_2$, respectively. The Rigaku CrystalClear (version 1.3.6) program package was utilized for diffraction image collection and the area detector data process. Lorentz and polarization corrections were also applied to data reduction.

Both structures of $\text{BaM}(\text{BS}_3)_2$ (M = Sb, Bi) were solved by direct methods and refined by full matrix least-squares on F^2 using the SHELXL-97 package.¹⁴ Their lattice types and space groups were suggested by systematic absence conditions of the collected data. The program PLATON was used to check the final refined crystal structures of $\text{BaM}(\text{BS}_3)_2$ (M = Sb, Bi), and no missed symmetry elements were found. X-ray energy dispersive spectroscopy (EDS, Oxford INCA) analysis on a field emission scanning electron microscope (FESEM, JSM6700F) also confirmed a Ba/M/S molar ratio of 1.00:1.05:4.04 (for M = Sb) and 1.00:1.04:3.90 (for M = Bi), which are in good agreement with stoichiometric proportions from their single crystal X-ray structural analyses. As EDS analysis is unable to give proper spectroscopy values for elements lighter than boron, IR spectra were performed on an FR-IR spectrometer, confirming the presence of BS_3 groups and elemental boron. The crystallographic data, atomic coordinates, and selected bond distances for $\text{BaM}(\text{BS}_3)_2$ (M = Sb, Bi) are summarized in Tables 1–3.

Powder X-ray diffraction patterns of both compounds were recorded on a Rigaku MiniFlex II diffractometer with Cu $K\alpha$ radiation. The scanning range is $5\text{--}85^\circ$ in 2θ with a step size of 0.01° and an exposure time of 0.16 s. The experimental powder XRD patterns of $\text{BaM}(\text{BS}_3)_2$ (M = Sb, Bi) are shown in the Supporting Information (Figures S1 and S2), indicating good agreement with those calculated from the final refined single crystal data.

Infrared and UV–vis Diffused Reflectance Spectroscopy. The infrared spectra of $\text{BaM}(\text{BS}_3)_2$ (M = Sb, Bi) were recorded on a PerkinElmer Spectrum One FR-IR spectrometer in the range of $450\text{--}4000 \text{ cm}^{-1}$ for the samples diluted with dry KBr and pressed into translucent pellets. The UV–vis diffuse reflectance

(9) Stoltzfus, M. W.; Woodward, P. M.; Seshadri, R.; Klepeis, J. H.; Bursten, B. *Inorg. Chem.* **2007**, *46*, 3839.

(10) Zhang, W. L.; Lin, X. S.; Zhang, H.; Wang, J. Y.; Lin, C. S.; He, Z. Z.; Cheng, W. D. *Dalton. Trans.* **2010**, *39*, 1546.

(11) Barbier, J.; Penin, N.; Denoyer, A.; Cranswick, L. M. D. *Solid State Sci.* **2005**, *7*, 1055.

(12) Dösch, M.; Hammerschmidt, A.; Krebs, B. *Z. Anorg. Allg. Chem.* **2004**, *630*, 519.

(13) Hammerschmidt, A.; Dösch, M.; Püttmann, C.; Krebs, B. *Z. Anorg. Allg. Chem.* **2003**, *629*, 551.

(14) Sheldrick, G. M. *SHELXTL-97*; University of Göttingen: Göttingen, Germany, 1997.

Table 2. Atomic Coordinates and Equivalent Isotropic Displacement Parameters (\AA^2) for Compounds $\text{BaM}(\text{BS}_3)\text{S}$ ($M = \text{Sb, Bi}$)

| atom | x | y | z | $U(\text{eq})^a$ |
|------------------------------|-----------|------------|-------------|------------------|
| BaSb(BS₃)S | | | | |
| Ba(1) | 0.4863(1) | 0.2500 | 0.6690(1) | 0.015(1) |
| Sb(1) | 0.8110(1) | 0.2500 | 0.4597(1) | 0.014(1) |
| B(1) | 0.1912(3) | 0.2500 | 0.4514(3) | 0.011(1) |
| S(1) | 0.7934(1) | −0.0014(1) | 0.6292(1) | 0.015(1) |
| S(2) | 0.5731(1) | 0.2500 | 0.4075(1) | 0.015(1) |
| S(3) | 0.1702(1) | 0.2500 | 0.6019(1) | 0.018(1) |
| BaBi(BS₃)S | | | | |
| Ba(1) | 0.3191(1) | −0.5000 | 0.13077(1) | 0.013(1) |
| Bi(1) | 0.4535(1) | 0 | 0.7427(1) | 0.014(1) |
| B(1) | 0.3969(9) | −0.5000 | 0.18444(17) | 0.010(3) |
| S(1) | 0.3411(2) | 0 | 0.4503(4) | 0.016(1) |
| S(2) | 0.4658(2) | −0.5000 | 0.6805(4) | 0.015(1) |
| S(3) | 0.3596(1) | 0.2514(4) | 0.19312(3) | 0.014(1) |

^a $U(\text{eq})$ is defined as one-third of the trace of the orthogonalized U_{ij} tensor.

Table 3. Bond Lengths (\AA) and Angles (deg) for Compounds $\text{BaM}(\text{BS}_3)\text{S}$ ($M = \text{Sb, Bi}$)

| | | | |
|------------------------------|------------|--------------------|------------|
| BaSb(BS₃)S | | | |
| Ba(1)–S(3) | 3.1620(10) | Ba(1)–S(1) × 2 | 3.3943(7) |
| Ba(1)–S(2) | 3.1651(10) | Sb(1)–S(2) | 2.3837(9) |
| Ba(1)–S(3) | 3.2122(9) | Sb(1)–S(1) × 2 | 2.5290(7) |
| Ba(1)–S(2) × 2 | 3.2910(7) | B(1)–S(1) × 2 | 1.818(2) |
| Ba(1)–S(1) × 2 | 3.3896(7) | | |
| S(2)–Sb(1)–S(1) × 2 | 97.73(2) | S(3)–B(1)–S(1) × 2 | 121.55(10) |
| S(1)–Sb(1)–S(1) | 76.51(3) | S(1)–B(1)–S(1) | 116.8(2) |
| BaBi(BS₃)S | | | |
| Ba(1)–S(2) | 3.206(3) | Ba(1)–S(3) × 2 | 3.402(2) |
| Ba(1)–S(2) | 3.208(3) | Bi(1)–S(1) | 2.495(3) |
| Ba(1)–S(1) | 3.298(3) | Bi(1)–S(3) × 2 | 2.699(2) |
| Ba(1)–S(1) × 2 | 3.2985(10) | B(1)–S(3) × 2 | 1.817(7) |
| Ba(1)–S(3) × 2 | 3.310(2) | | |
| S(1)–Bi(1)–S(3) × 2 | 97.86(8) | S(2)–B(1)–S(3) × 2 | 121.3(3) |
| S(3)–Bi(1)–S(3) | 71.15(9) | S(3)–B(1)–S(3) | 117.4(7) |

spectra were measured on a PerkinElmer Lambda 900 UV/vis spectrometer equipped with an integrating sphere over the 200–2000 nm wavelength range at room temperature. A BaSO_4 plate was used as reference material (100% reflectance). The optical absorption spectra of powder samples were converted from diffuse reflectance spectra using the Kubelka–Munk function, $\alpha/S = (1 - R)^2/2R$, where R is the diffuse reflectance and α and S are the Kubelka–Munk absorption and scattering coefficients.^{15,16}

Electronic Structure Calculations. We performed electronic energy band structure calculations to give further understanding and interpretation of the electrical and optical properties of the compounds synthesized. The crystallographic data of $\text{BaM}(\text{BS}_3)\text{S}$ ($M = \text{Sb, Bi}$) determined by the single crystal X-ray diffraction method were used for band structure calculations, and no further geometry optimizations were performed. The band structure calculations of the two compounds were performed by using the first-principles quantum mechanical program CASTEP within the density functional theory (DFT) formalism.¹⁷ Pseudopotentials were utilized to describe electron–ion interactions, and a plane-wave basis set was used to represent electronic wave functions in the CASTEP program. The

exchange–correlation potential was calculated using the Perdew–Burke–Ernzerhof (PBE) function within the generalized gradient approximation (GGA) scheme.¹⁸ Norm-conserving pseudopotentials were employed for all of the atoms in the reciprocal space representation.¹⁹ The Monkhorst–Pack²⁰ k -point grid sampling with $3 \times 4 \times 2$ for $\text{BaSb}(\text{BS}_3)\text{S}$ and $4 \times 4 \times 3$ for $\text{BaBi}(\text{BS}_3)\text{S}$ was applied in the DFT calculations. Energy cutoffs of 450 and 400 eV were used to determine the plane wave basis sets for $\text{BaSb}(\text{BS}_3)\text{S}$ and $\text{BaBi}(\text{BS}_3)\text{S}$, respectively. Pseudo atomic calculations were performed for B $2s^2 2p^1$, S $3s^2 3p^4$, Sb $5s^2 5p^3$, Bi $5d^{10} 6s^2 6p^3$, and Ba $5s^2 5p^6 6s^2$. The rest of the parameters used in the calculations were set by the default values of the CASTEP code.

Results and Discussion

Synthesis. The two new thioborates $\text{BaSb}(\text{BS}_3)\text{S}$ (colorless) and $\text{BaBi}(\text{BS}_3)\text{S}$ (orange yellow) with strongly one-dimensional growth along crystallographic b direction were obtained using the conventional solid state reaction method in vacuumized quartz tubes. Throughout the experiments, carbon crucibles were used as containers to ensure that B_2S_3 had almost no reaction with silicon dioxide, and therefore the yields could reach more than 90%. Needle-like single crystals were selected carefully and grinded into powder for further experiments. The procedure of how to set the temperature is vital for the successful synthesis of thioborates. Byproducts, such as Ba_2SiS_4 , would be found if the temperature is too high or the time of constant temperature too long within an inappropriate temperature range. Experiments demonstrate that it is necessary to hold it about 20 h at 800 K and no more than 10 h at 1100 K, which can reduce the reaction of B_2S_3 with SiO_2 . Powder X-ray diffraction patterns of compounds $\text{BaSb}(\text{BS}_3)\text{S}$ and $\text{BaBi}(\text{BS}_3)\text{S}$ are in good agreement with the calculated ones on the basis of their previously determined single crystallographic structures, showing no presence of other impure phases (Figures S1 and S2 in the Supporting Information).

Crystal Structures. The two compounds of $\text{BaM}(\text{BS}_3)\text{S}$ ($M = \text{Sb, Bi}$) both crystallize in one-dimensional chain-like structures which are built up of $[\text{BS}_3]^{3-}$ trigonal plane rings alternately bridged by $[\text{MS}_3]^{3-}$ ($M = \text{Sb, Bi}$) trigonal pyramids via sulfur atoms shared along the crystallographic b axis (Figure 1). The polymeric chains of $\text{MS}_3\text{–BS}_3$ (which can also be written in the form of $[\text{MBS}_4]^{2-}$, $M = \text{Sb, Bi}$) are parallel to each other with barium atoms inserted among four neighbored chains, forming whole crystal structures via electrostatic forces between Ba^{2+} cations and $[\text{MBS}_4]^{2-}$ anionic polymeric chains (Figure 2). Although the two compounds have similar structural units of $[\text{MBS}_4]^{2-}$ polymeric chains, they crystallize in different space groups. $\text{BaSb}(\text{BS}_3)\text{S}$ crystallizes in $Pnma$ of the orthorhombic system with unit cell parameters of $a = 9.6898(15)$ \AA , $b = 6.2293(13)$ \AA , $c = 11.670(2)$ \AA , $V = 704.4(2)$ \AA^3 , and $Z = 4$, while $\text{BaBi}(\text{BS}_3)\text{S}$ crystallizes in space group $C2/m$ with unit cell parameters of $a = 14.9890(17)$ \AA , $b = 6.2457(6)$ \AA , $c = 7.5591(9)$ \AA , $\beta = 101.604(5)^\circ$, $V = 693.19(13)$ \AA^3 , and $Z = 4$. Besides the three sulfur atoms

(15) Wendlandt, W. W.; Hecht, H. G. *Reflectance Spectroscopy*; Interscience: New York, 1966.

(16) Kortüm, G., *Reflectance Spectroscopy*; Springer-Verlag: New York, 1969.

(17) Clark, S. J.; Segall, M. D.; Pickard, C. J.; Hasnip, P. J.; Probert, M. J.; Refson, K.; Payne, M. C. *Z. Kristallogr.* **2005**, *220*, 567.

(18) Perdew, J. P.; Burke, K.; Ernzerhof, M. *Phys. Rev. Lett.* **1996**, *77*, 3865.

(19) Payne, M. C.; Teter, M. P.; Allan, D. C.; Arias, T. A.; Joannopoulos, J. D. *Rev. Mod. Phys.* **1992**, *64*, 1045.

(20) Pack, J. D.; Monkhorst, H. J. *Phys. Rev. B.* **1977**, *16*, 1748.

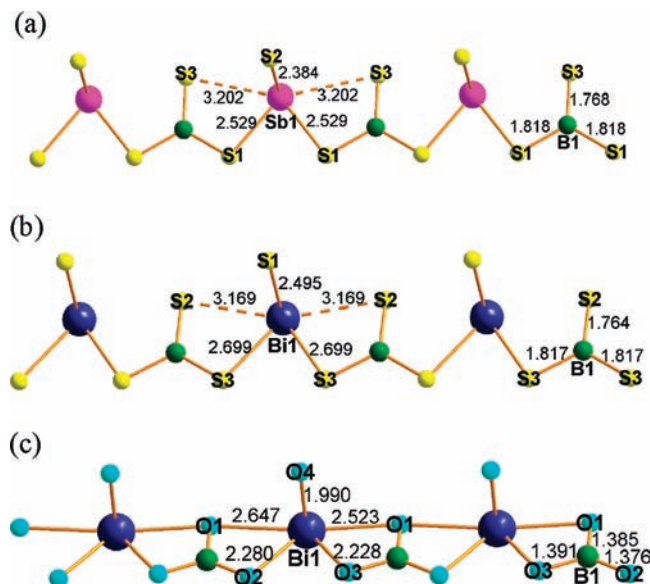


Figure 1. (a) Structure unit of $[\text{SbBS}_4]^{2-}$ polymeric chain and antimony and boron cation environments for $\text{BaSb}(\text{BS}_3)\text{S}$. (b) Structure unit of $[\text{BiBS}_4]^{2-}$ polymeric chain and bismuth and boron cation environments for $\text{BaBi}(\text{BS}_3)\text{S}$. (c) $[\text{BiBO}_4]^{2-}$ one-dimensional chain structure along c axis direction and coordination environments of bismuth and boron in BaBiBO_4 for comparison.

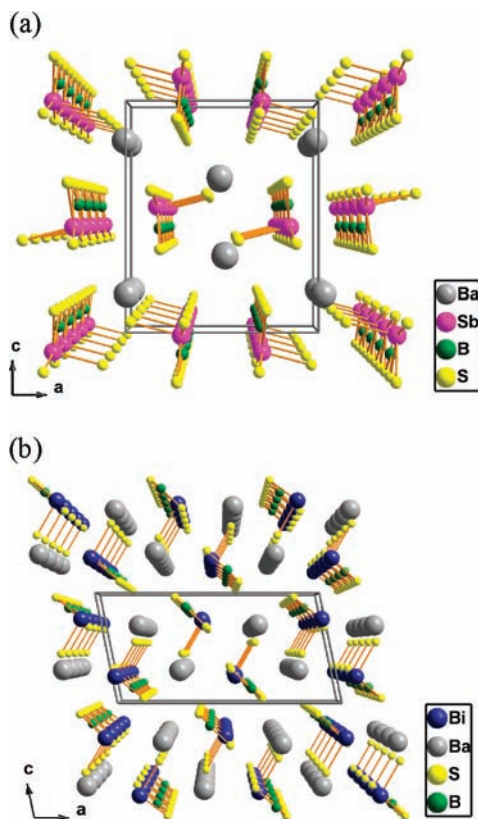


Figure 2. (a) Crystal structure of $\text{BaSb}(\text{BS}_3)\text{S}$ viewed along the b axis. (b) Crystal structure of $\text{BaBi}(\text{BS}_3)\text{S}$ viewed along the b axis.

coordinating at the MS_3 trigonal-pyramidal vertices (bond length ranging from 2.3838 to 2.5291 Å for antimony and 2.4951 to 2.6990 Å for bismuth atoms), there are two next nearest neighbors with distances of 3.202 Å for antimony and 3.169 Å for bismuth atoms (Figure 1). The Ba^{2+} cations

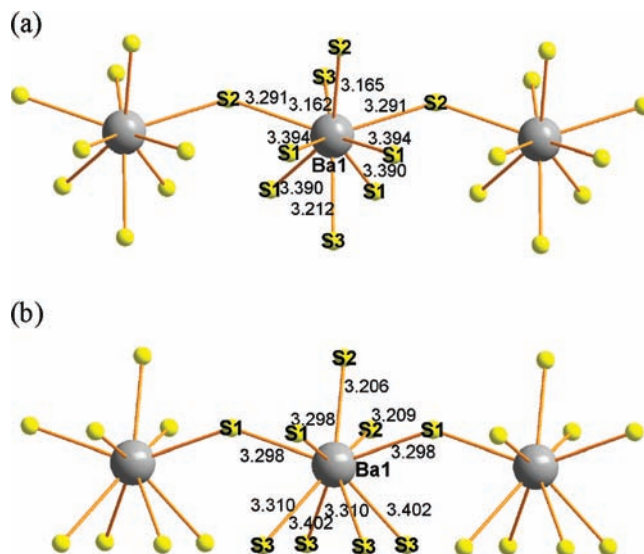


Figure 3. Barium cation environments and distances to nine nearest sulfide atoms for (a) $\text{BaSb}(\text{BS}_3)\text{S}$ and (b) $\text{BaBi}(\text{BS}_3)\text{S}$.

have a typical coordination environment with nine sulfur atoms at distances of 3.162–3.3943 Å for $\text{BaSb}(\text{BS}_3)\text{S}$ and 3.2060–3.4023 Å for $\text{BaBi}(\text{BS}_3)\text{S}$ (Figure 3). Boron atoms have typical trigonal plane coordinations with three sulfide atoms, and the bond lengths range from 1.770(4) to 1.818(2) Å for $\text{BaSb}(\text{BS}_3)\text{S}$ and 1.765(13) to 1.817(7) Å for $\text{BaBi}(\text{BS}_3)\text{S}$, which are in accordance with values reported previously in the literature.^{2,13,21} The bond angles of S–B–S slightly deviate away from 120° as a result of the asymmetrical coordination environment of $[\text{BS}_3]^{3-}$ anions, while the sum of S–B–S bond angles is exactly equal to 360° , which indicates a planar $[\text{BS}_3]^{3-}$ structure in both of the compounds, $\text{BaSb}(\text{BS}_3)\text{S}$ and $\text{BaBi}(\text{BS}_3)\text{S}$.

Bond-valence sums of Sb^{3+} and Bi^{3+} cations give reasonable oxidation states of 3.07 and 2.87, Ba^{2+} gives sums of 2.23 and 2.16, and B^{3+} gives sums of 3.16 and 3.18 for $\text{BaSb}(\text{BS}_3)\text{S}$ and $\text{BaBi}(\text{BS}_3)\text{S}$, respectively, using the bond-valence parameters summarized by Brown and Altermatt and Brese and O’Keeffe.^{22,23} The calculated ones are in good agreement with normal oxidation states of 3, 2, and 3 for Sb^{3+} (Bi^{3+}), Ba^{2+} , and B^{3+} cations in the two compounds. According to the bond-valence values of Sb^{3+} or Bi^{3+} cations, summarized in Table S1 in the Supporting Information, most of the bond-valence values are distributed over the three nearest S atoms, and the two farther S atoms have less contribution to the cations’ oxidation state values. Accordingly, we can suppose the $[\text{MS}_3]^{3-}$ ($\text{M} = \text{Sb}, \text{Bi}$) trigonal-pyramidal units are formed as one relatively stabilized component of the $\text{MS}_3\text{--BS}_3$ ($\text{M} = \text{Sb}, \text{Bi}$) polymer in the crystal structures.

It is meaningful to make comparisons between the $\text{BaM}(\text{BS}_3)\text{S}$ ($\text{M} = \text{Sb}, \text{Bi}$) compounds and BaBiBO_4 ,¹¹ as they have similar one-dimensional chain structures. The latter compound crystallizes in a noncentrosymmetric space group ($\text{Pna}2_1$) and exhibits about 5 times

(21) Hammerschmidt, A.; Jansen, C.; Küper, J.; Köster, C.; Krebs, B. *Z. Anorg. Allg. Chem.* **2001**, *627*, 669.

(22) Brown, I. D.; Altermatt, D. *Acta Crystallogr., Sect. B: Struct. Sci.* **1985**, *41*, 244.

(23) Brese, N. E.; O’Keeffe, M. *Acta Crystallogr., Sect. B: Struct. Sci.* **1991**, *47*, 192.

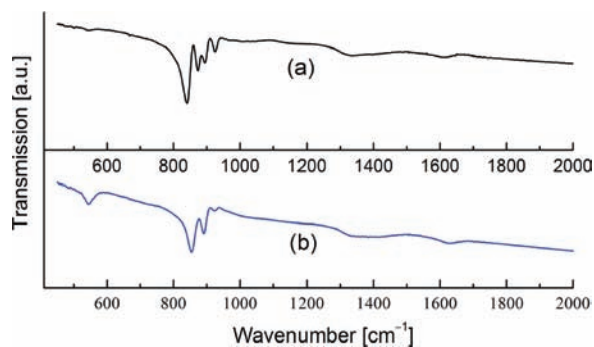


Figure 4. Infrared transmission spectra of $[\text{BS}_3]^{3-}$ units for polycrystalline samples of (a) $\text{BaSb}(\text{BS}_3)\text{S}$ and (b) $\text{BaBi}(\text{BS}_3)\text{S}$.

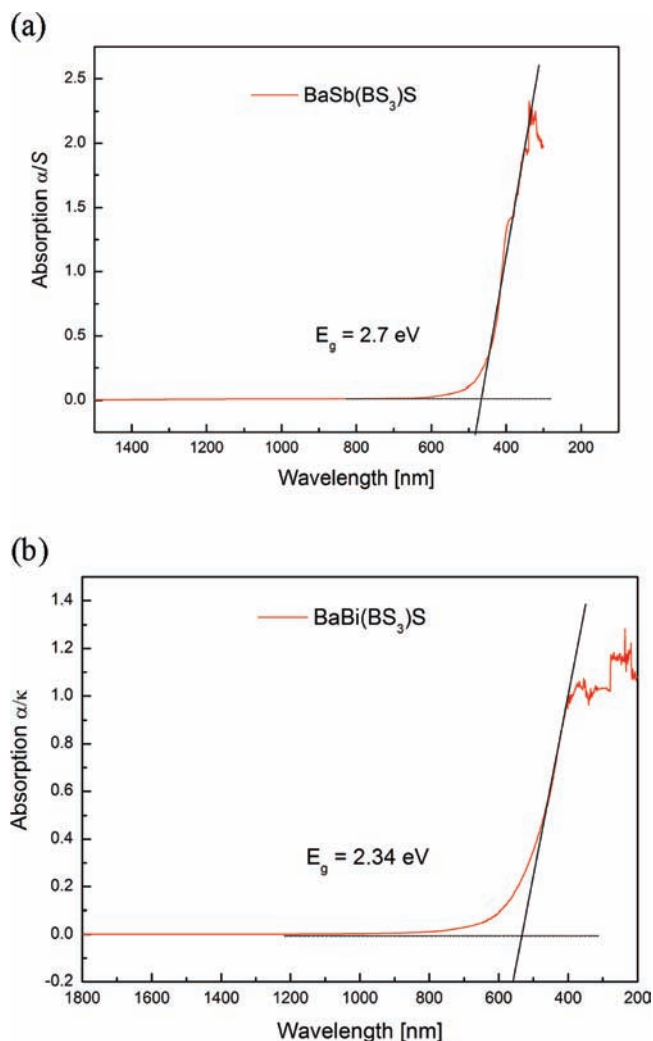


Figure 5. Optical absorption spectra converted using Kubelka–Munk function from diffuse reflectance spectra for powder samples of (a) $\text{BaSb}(\text{BS}_3)\text{S}$ and (b) $\text{BaBi}(\text{BS}_3)\text{S}$.

the SHG efficiency of KDP,¹¹ while the former two compounds both crystallize in centrosymmetric space groups and have no SHG response. In the $[\text{MBS}_4]^{2-}$ chain structures, as shown in Figure 1a and b, $[\text{MS}_5]$ is a tetragonal pyramid with a mirror plane across the M atom and perpendicular to the chain direction, while in the $[\text{BiBO}_4]^{2-}$ chain, as shown in Figure 1c, the $[\text{BiO}_5]$ is a distorted polyhedron with no mirror plane perpendicular to the chain direction, resulting in a noncentrosymmetric

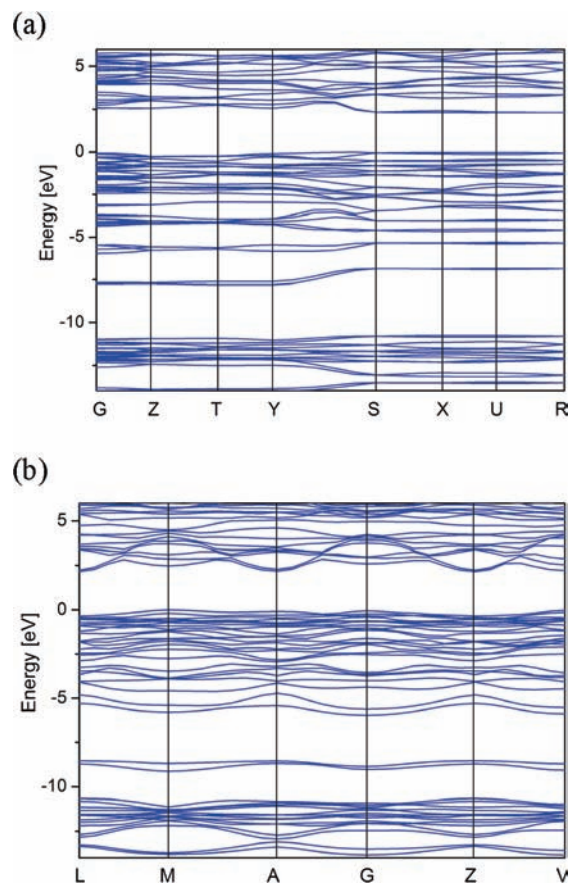


Figure 6. Electronic band structures of (a) $\text{BaSb}(\text{BS}_3)\text{S}$ and (b) $\text{BaBi}(\text{BS}_3)\text{S}$.

space group of the latter compound. Accordingly, when the O atom is replaced by the S atom in the Ba–M–B–O system, an acentric space group of the compound is lost due to the fact that a large-sized S atom might change the coordination environments of the M ions.

Optical Properties of $\text{BaM}(\text{BS}_3)\text{S}$ ($\text{M} = \text{Sb}, \text{Bi}$). Infrared spectra also illustrate the possible vibration modes of $[\text{BS}_3]^{3-}$ units in both compounds (Figure 4). Strong phonon absorption around 850 cm^{-1} and weak absorption around 450 cm^{-1} could be assigned to the asymmetrical stretching E modes and the symmetrical A_1' modes of the $[\text{BS}_3]^{3-}$ unit, respectively, with a point symmetry group of D_{3h} . The IR absorption spectra of the two titled compounds are in accordance with those of other thioborates published previously.^{1,4,8,24–26} It is notable that the angles of S–B–S slightly deviated from 120° make the point group symmetry of $[\text{BS}_3]^{3-}$ reduce its degree of degeneracy from D_{3h} to C_{2v} , resulting in the appearance of weak vibration modes around $850\text{--}950\text{ cm}^{-1}$.

Figure 5a and b show the optical reflectance spectrum measurement results, indicating that both compounds $\text{BaSb}(\text{BS}_3)\text{S}$ and $\text{BaBi}(\text{BS}_3)\text{S}$ are semiconductors with optical band gaps of 2.70 and 2.34 eV, respectively. The band gap of $\text{BaSb}(\text{BS}_3)\text{S}$ is larger than that of $\text{BaBi}(\text{BS}_3)\text{S}$, which features a similar tendency to the results

(24) Hiltmann, F.; Krebs, B. *Z. Anorg. Allg. Chem.* **1995**, 621, 424.

(25) Royle, M.; Cho, J.; Martin, S. W. *J. Non-Cryst. Solids* **2001**, 279, 97.

(26) Cho, J.; Martin, S. W. *J. Non-Cryst. Solids* **2002**, 298, 176.

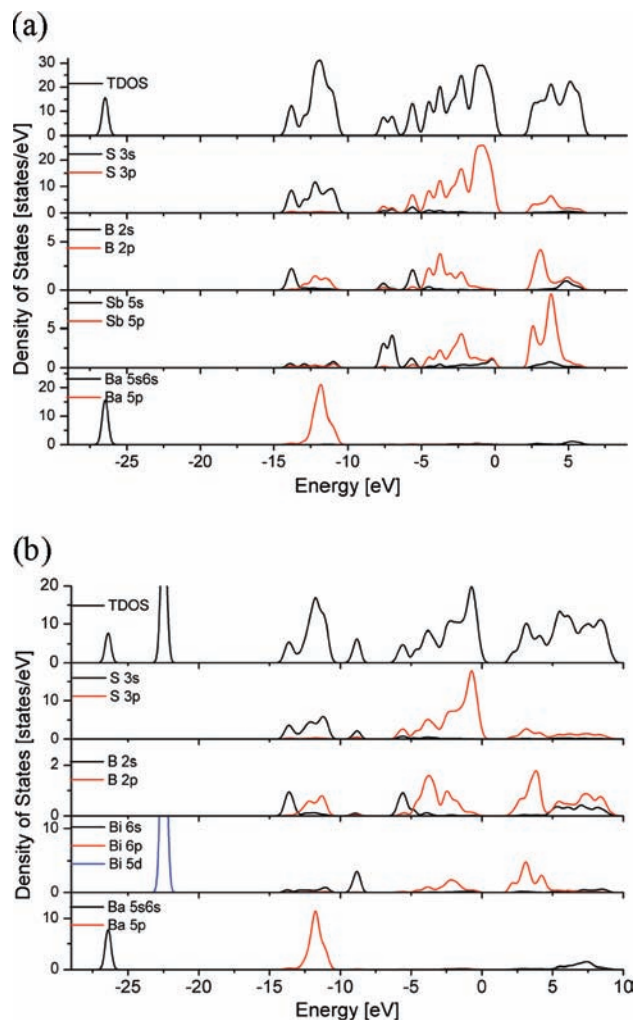


Figure 7. Total and PDOS of (a) BaSb(BS₃)S and (b) BaBi(BS₃)S.

of electronic band structure calculations reported in the next section.

Band Structures and Density of States. The band structures of BaSb(BS₃)S and BaBi(BS₃)S along high symmetry points of the first Brillouin zone (BZ) are shown in Figure 6a and b. The special *k* points in the first BZ are defined in Table S2 in the Supporting Information. The valence band maximum (VBM) and the conduction band minimum (CBM) are located at the YS line near the S point and the XU line near the U point of the Brillouin zone with a band gap of 2.29 eV for BaSb(BS₃)S, and the M and L points with a band gap of 2.16 eV for BaBi(BS₃)S, respectively, indicating that both of them belong to indirect band gap semiconductors. In addition, we have the experimental absorption edges of the two compounds, according to the optical diffuse reflectance spectrum measurements. The calculated energy gaps are slightly smaller than the measured values, 2.70 and 2.34 eV for BaSb(BS₃)S and BaBi(BS₃)S respectively, just as expected from the DFT method, and the band gap is generally underestimated due to insufficient accuracy of the exchange correlation energy calculated.²⁷ Comparing the calculated energy gaps with the experimented ones, we can see that the results of our calculation are good and

give reasonable explanations for the optical absorption spectra.

Comparing Figure 6a with b and Figure 7a with b, we can see that their band structures and densities of state exhibit much resemblance, due to both of them being constituted of similar MS₃–BS₃ polymeric chain units. Therefore, only the partial densities of state (PDOS) for BaSb(BS₃)S will be discussed in detail as a representative. The band structure and the PDOS can be divided into four major distinct regions, as can be seen from Figures 6a and 7a. The lowest part located around –27.0 eV is contributed by an inner Ba-5s orbital with a very sharp and narrow shape. The next region, ranging from –15.0 to –10.0 eV, is mainly composed of S-3s, Ba-5p, and B-2s2p states with a small mixture of Sb-5s states. The third region extends in a wide range from –8.0 eV to VBM, i.e., the Fermi level. This band mostly originates from S-3p states with some mixing of B-2p and Sb-5p states. The component at VBM is mainly composed of S-3p states and a small amount of Sb-5p states. It is worth noting that strong hybridizations occur between the Sb–S bonding states and B–S bonding states in the range of –8.0 to –2.0 eV. The last band region situated around 2.5 to 6.0 eV, which constitutes the conduction band, has significant contributions from the mixings of the antibonding states between Sb-5p and S-3p states with the antibonding states between B-2p and S-3p states. While near the lowest conduction band, Sb-5p states are the main components. Accordingly, the absorption spectrum near the UV–visible cutoff wavelength can be assigned as the charge transfers from S-3p states to Sb-5p (Bi6p) states for BaSb(BS₃)S and BaBi(BS₃)S compounds.

Conclusions

We have synthesized and characterized two new quaternary thioborate compounds, BaSb(BS₃)S and BaBi(BS₃)S, which crystallize in isomorphous structures, although they belong to different space groups. To the best of our knowledge, they are the first quaternary compounds synthesized to date which incorporate antimony (or bismuth) atoms into thioborate and form strongly one-dimensional MS₃–BS₃ (M = Sb, Bi) polymeric chain structures by sharing [MS₃]^{3–} trigonal pyramids and [BS₃]^{3–} trigonal plane substructures alternatively. The IR absorption spectra performed on polycrystalline samples demonstrated the presence of [BS₃]^{3–} structural units in both compounds. UV–vis diffused reflectance spectroscopy measurements indicate that the band gap is 2.70 eV for BaSb(BS₃)S and 2.34 eV for BaBi(BS₃)S. The first-principles quantum mechanical calculations show that the two compounds are both indirect-gap semiconductors with band gaps of 2.29 and 2.16 eV, respectively, which is in good agreement with experimental values. The observed absorption peak from UV–vis diffused reflectance spectroscopy measurements is assigned as the charge transfers from S-3p states to Sb-5p (Bi6p) states in view of the calculations of band structures and densities of state for compounds BaSb(BS₃)S and BaBi(BS₃)S.

Acknowledgment. This investigation was based on work supported by the National Natural Science Foundation of China under project 20773131, the National Basic Research Program of China (No.2007CB815307), the Funds of Chinese Academy of Sciences (KJXC2-YW-H01,

(27) Godby, R. W.; Schluter, M.; Sham, L. J. *Phys. Rev. B* **1987**, *36*, 6497.

FJIRSM-SZD07001), and Fujian Key Laboratory of Nanomaterials (No. 2006L2005).

Supporting Information Available: X-ray crystallographic files in CIF format, simulated and experimental powder X-ray

diffraction patterns for BaSb(BS₃)S (Figure S1) and BaBi(BS₃)S (Figure S2), selected bond-valence sums for the two titled compounds (Table S1), and the definitions of the special *k*-points in the first Brillouin zone (Table S2). These materials are available free of charge via the Internet at <http://pubs.acs.org>.